Analysis of wave energy device dynamics and power optimization

Chen Li *

School of Intelligent Manufacturing, Nanjing University of Science and Technology, Wuxi, Jiangsu, 214443

* Corresponding author: chen040724@gmail.com

Abstract. As an important renewable resource, wave energy has considerable development value and application prospects. How to design a wave energy conversion device to maximize the output power is an urgent problem in its practical application. In this paper, we mainly study the principle of wave energy device capacity, the motion and power model of the constructed wave energy device, and finally design a specific scheme to achieve the maximum output power of wave energy through kinetic analysis, the fourth-order ordinary differential equation solved by the Longacurta method, and the Simpson integral method. At the end of the paper, the developed model is objectively evaluated and the potential value of the developed model in practical wave energy device applications is illustrated.

Keywords: kinetic analysis, Longacurta method, Simpson integral method.

1. Introduction

The level of power consumption is an important indicator to measure the development degree of society [1]. Electricity generation will account for over half of global energy consumption by the middle of this century, while the global energy system is gradually facing severe challenges, and the development and utilization of renewable energy has become a hot topic in today's society. Wave energy is a kind of clean renewable energy [2], and its development and utilization is of great significance to alleviate the energy crisis and reduce carbon emissions. At the same time, its energy conversion device mainly adopts the wave energy-mechanical energy-electric energy conversion method, which is relatively simple. Most of the wave energy converter(WEC) devices are either fixed on the shore or near the shore, or float on the water surface or in the water body by anchoring [3], with the type roughly divided into oscillating water column type, surfing wave type and vibrating float type, based on different working principles [4]. There are many key technologies for wave power generation, and control technology has always been the core of engineering applications and a hot research topic for experts and scholars [5]. In this paper, we mainly study the principle of wave energy device capacity with the type of vibrating float which has a oscillating in the float. The water level of the whole motion process is discussed first, and the conical part of the float is judged not to be higher than the sea level, so as to put forward reasonable assumptions for the calculation of subsequent problems. Since only the vertical swing motion is considered, only the kinematic analysis in the vertical direction is required. The force analysis of the float and the oscillator in the device is carried out separately, and a set of differential equations is established by applying Newton's second law, which is transformed and simplified into a fourth-order ordinary differential equation, and the numerical solution is solved by using the Longacurta method. In addition, this paper considers that the float and the oscillator do oscillation motion, and assumes and verifies that the longitudinal oscillation motion is small angle motion, so it does not affect the pendular motion, so the oscillation motion is decomposed into pendular and longitudinal oscillation motion separately. Finally, The angular displacement and angular velocity of the float and oscillator are given.

2. Model establishment and solution

2.1. Float initial state analysis

The float and the oscillator are balanced in the static water at the initial moment, because the float is composed of a cylindrical shell with uniform mass distribution and conical shell, so the height of the initial water level has a certain influence on its initial state of buoyancy. Then we can divide it into the following two cases to discuss, the first case is the height where the water level is at the conical surface position, and the second case is the height where the water level reaches the cylindrical surface position.

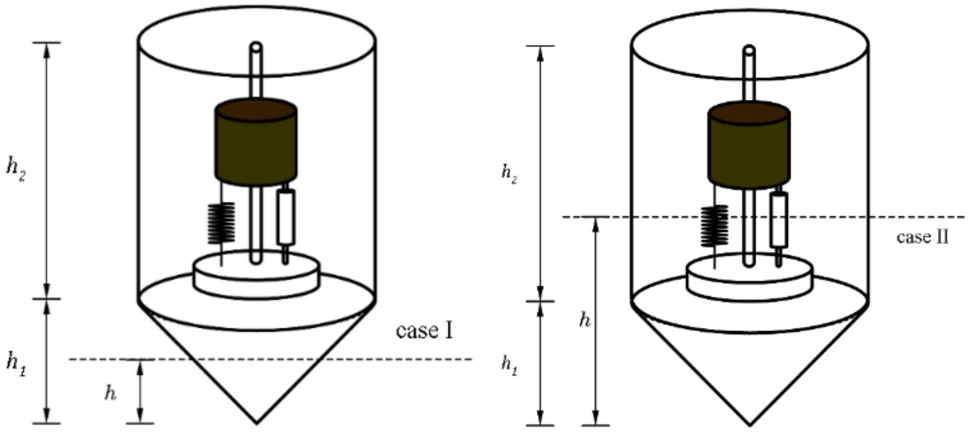

Figure 1. Initial water level map

The buoyant force on the object is equal to the gravitational force of the liquid discharged, and the initial case one corresponds to the formula for buoyancy.

$$V = \frac{m_o+m_f}{\rho} = \frac{\pi}{3} \cdot (\frac{hR_f}{h_1})^2 \cdot h \tag{1}$$

The initial case II corresponds to the buoyancy force of Eq.

$$V = \frac{m_o+m_f}{\rho} = \frac{\pi}{3} \cdot {R_f}^2 \cdot h_1 + \pi {R_f}^2 (h - h_1) \tag{2}$$

After substituting the corresponding parameters, it is calculated that the initial equilibrium state, h=2.8m, corresponds to the initial case II, and the water level height is still enough distance from the cone surface part to expose the sea level. Therefore, we can make the assumption that the cone surface will not be exposed to the sea level when the float does the vertical swinging motion.

2.2. Hydrodynamic analysis of wave energy device

According to the hydrodynamic theory of wave energy generation device [6] [7], the equation of motion of the oscillating float with single degree of freedom lifting and sinking motion can be expressed as

$$(m_f + A)\ddot{x}_f = F_d - B\dot{x}_f - \rho g S x_f + F_{PTO} \tag{3}$$

Where m_f is the mass of the float itself; x_f is the displacement of the oscillator with respect to the initial equilibrium position; F_d is the excitation force in the vertical direction; A represents the additional mass of the float moving in the fluid and driving the surrounding fluid together; B is the hinged wave damping coefficient generated with the moving fluid; $--\rho g S x$ is the hydrostatic recovery force; F_{PTO} is the power takeoff device (PTO) acting in the direction of the float pendulum F_{PTO} is the load of the power takeoff device (PTO) acting on the float in the pendulum direction, which contains the damping force of the linear damper and the force of the linear spring. The force analysis of the float in the pendulum motion is shown in the figure 2 below.

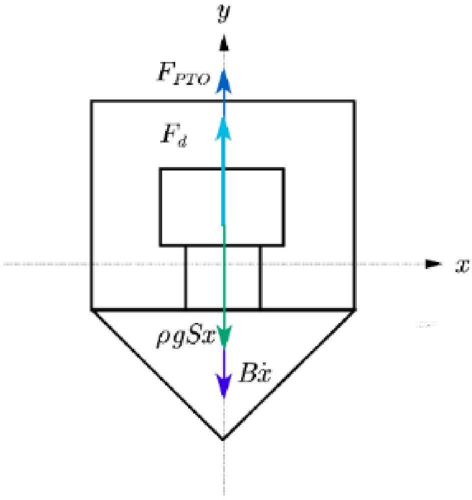

Figure 2. Float force analysis

By the definition of F_{PTO}, its expression can be obtained as follows

$$F_{PTO} = -C(\dot{x_f} - \dot{x_o}) - K(x_f - x_o) \tag{4}$$

Where x_o is the displacement of the oscillator with respect to the initial equilibrium position, C is the damping coefficient of the damper, and K is the spring stiffness. The wave excitation force F_d is given in the title as $fcoswt$ (f is the wave excitation force amplitude, w is the wave frequency). Substituting it into equation (3), the obtained expression for the float motion is as follows

$$(m_f + A)\ddot{x_f} = fcoswt - B\dot{x_f} - \rho g \pi {R_f}^2 x_f - C(\dot{x_f} - \dot{x_o}) - K(x_f - x_o) \tag{5}$$

The force analysis diagram of the oscillator is shown below. During the motion of the oscillator, it is subject to three forces, which are the gravity of the oscillator itself, the spring force on the oscillator, and the force of the damper on the oscillator.

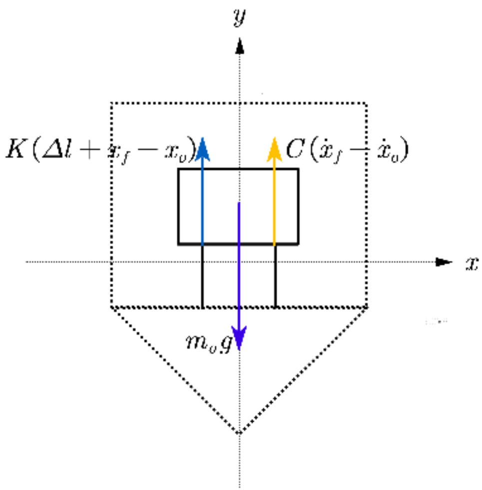

Figure 3. Force analysis of oscillator

Where Δl is the spring compression at the initial moment and $x_f - x_o$ is the increment of the spring compression during the dangling motion. By the initial equilibrium state, the equilibrium equation $k\Delta l = m_o g$ is obtained, and then the analysis of the oscillator dynamics leads to the following expression.

$$m_o\ddot{x_o} = C(\dot{x_f} - \dot{x_o}) + K(x_f - x_o) = F_{PTO} \tag{6}$$

Combining the two equations (5) (6), eliminating the variable x_o and simplifying it, the fourth order ordinary differential equation can be obtained.

$$(m_f + A){x_f}^{(4)} = (\frac{Kf}{m_o} - fw^2)coswt - \frac{Cfw}{m_o}sinwt - (B + C + \frac{C(m_f + A)}{m_o})\dddot{x_f} - [\rho g\pi {R_f}^2 + K + \frac{BC+K(m_f+A)}{m_o}]\ddot{x_f} - (\frac{C\rho g\pi {R_f}^2}{m_o} + \frac{KB}{m_o})\dot{x_f} - \frac{K\rho g\pi {R_f}^2}{m_o}x_f \tag{7}$$

2.3. Solving fourth-order ordinary differential equations using the Runge-Kutta method

The Runge-Kutta method (RK) is a class of implicit or explicit iterative methods for solving nonlinear ordinary differential equations, and is a high-precision single-step algorithm widely used in engineering. The algorithm is similar to the idea of Euler's method, which is an improvement of it and can be used to find numerical solutions of differential equations. This algorithm takes measures to suppress errors and has high accuracy. The principle of its implementation is as follows

Suppose$\dot{y} = f(x, y)$, $k_1 = f(x_n, y_n)$, then for the first-order accuracy of the Lagrangian median theorem we have

$$y(n + 1) - y(n) = f(x_n, y_n)(x_{n+1} - x_n) \tag{8}$$

The arithmetic mean of the slope approximation K_1 at point x_n and the slope K_2 at the right end point x_{n+1} is used as the approximation of the average slope K. Let $h = x_{n+1} - x_n$,the modified Lagrangian median theorem with second-order accuracy is obtained as follows

$$\begin{cases} y(n + 1) - y(n) = \frac{1}{2}h(K_1 + K_2) \\ K_1 = f(x_n, y_n) \\ K_2 = f(x_n + h, y_n + h \cdot K_1) \end{cases} \tag{9}$$

By analogy, if the slope values K_1, K_2, ……K_m at multiple points are predicted in the interval $[x_n,x_{n+1}]$ and their weighted averages are used as the approximation of the average slope K, a higher-order formula with higher accuracy can be constructed. After a derivation similar to the above, the fourth-order Longacurta formula can be derived, which is shown in the following form.

$$\begin{cases} y(n + 1) - y(n) = \frac{1}{6}h(K_1 + 2K_2 + 2K_3 + K_4) \\ K_1 = f(x_n, y_n) \\ K_2 = f(x_n + \frac{h}{2}, y_n + \frac{1}{2}hk_1) \\ K_3 = f(x_n + \frac{h}{2}, y_n + \frac{1}{2}hk_2) \\ K_4 = f(x_n + h, y_n + hk_3) \end{cases} \tag{10}$$

We use the Longacurta method, which is mainly applied when the derivative and initial value information of the equation is known[8][9], to simplify the complex process of finding the analytical solution of higher order ordinary differential equations using computer simulation.

First define the initial value of the state. Set the initial position as zero, the displacement of the float relative to the initial position x_f is 0; the whole system starts to move from the equilibrium state, the initial value of velocity is 0, and the initial value of acceleration is $\frac{f}{m_f+A}$. Since the acceleration produces an abrupt non-derivative at t=0, we replace the derivative with the difference to derive the initial value of the acceleration derivative at that point.

Based on the derivation of the kinematic equation above, the Longacurta formula for solving this differential equation can be written as follows

$$\begin{cases} Dx_f3 = x_f^{(4)} = \frac{1}{m_f+A} \cdot \{(\frac{Kf}{m_o} - fw^2) \cdot coswt - \frac{Cfw}{m_o} \cdot sinwt - [B + C + \frac{C\cdot(m_f+A)}{m_o}] \cdot Dx_f2 \\ -[\rho g\pi {R_f}^2 + K + \frac{BC}{m_o} + \frac{K(m_f+A)}{m_o}] \cdot Dx_f1 - (\frac{C\rho g\pi {R_f}^2}{m_o} + \frac{KB}{m_o}) \cdot Dx_f0 - (\frac{K\rho g\pi {R_f}^2}{m_o}) \cdot x_f\} \\ Dx_f2 = \dddot{x_f} \\ Dx_f1 = \ddot{x_f} \\ Dx_f0 = \dot{x_f} \end{cases} \tag{11}$$

Where Dx_f0 is the velocity of the float droop, Dx_f1 is the acceleration of the float droop, Dx_f2 is the first order derivative of the acceleration of the float droop with respect to time, and Dx_f3 is the second order derivative of the acceleration of the float droop with respect to time.

The solution of this system of equations utilizes the main idea of the Longacurta method: multiple specific points are selected in the vicinity of the target point t, and the function values of these points are linearly combined, using the combined values instead of the derivative values of point t in the Taylor expansion. The linear combination of the first-order derivative values of particular points in the interval is used to replace the nth-order derivative values at point t, in order to achieve the effect of predicting the power series expansion at a point by relying only on a series of first-order derivative values.

Starting from the initial time, i.e., from t=0, the iteration step of t is set to 0.1s, and the corresponding t values are substituted into the equation at each iteration, and the corresponding $\dot{x_f}$ and x_f are calculated by programming the multi-valued prediction, and their images with respect to t are drawn separately as follows

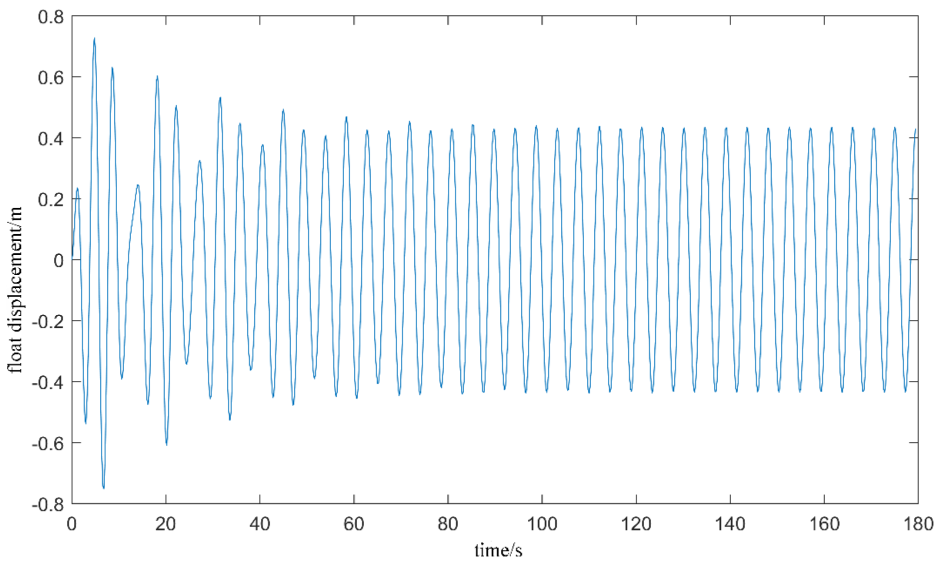

Figure 4. Float displacement vs. time

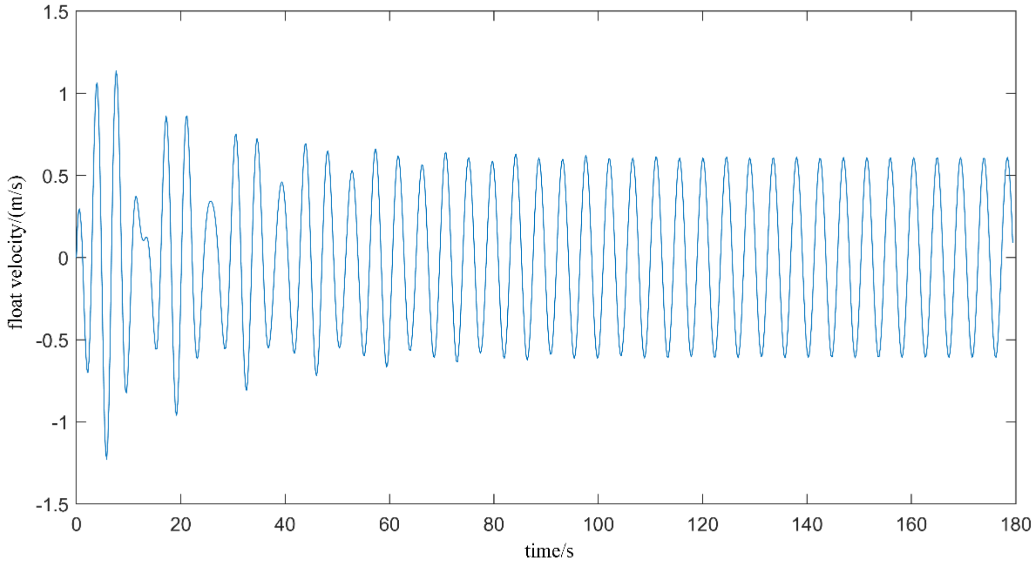

Figure 5. Float velocity vs. time

And Obtain the pendular displacement and velocity of the float at 10 s, 20 s, 40 s, 60 s and 100 s.

Table 1. pendular displacement and velocity of the float

Time	10s	20s	40s	60s	100s
float displacement (m)	-0.1944	-0.5934	0.2839	-0.3152	-0.0838
float velocity (m/s)	-0.6167	-0.2253	0.3194	-0.4768	-0.6038

By observing the maximum and minimum values in the x_f image, it can be determined that the lower half cone surface will not float out of the sea level during the float dangling motion, which verifies the reasonableness of the previous hypothesis.

Regarding the calculation of the oscillator displacement and velocity, the initial kinetic analysis of Eq. (5)(6) and the addition and subtraction transformations between the sets of equations lead to the following two equations regarding the oscillator displacement, velocity and float displacement.

$$\dot{x_o} = \frac{1}{m_o}[\frac{f}{w}sinwt - Bx_f - \rho g\pi {R_f}^2 \int_0^t x_f dt - (m_f + A)\dot{x_f}] \tag{12}$$

$$x_o = \frac{1}{m_o}[-\frac{f}{w^2}coswt + \frac{f}{w^2} - B\int_0^t x_f dt - \rho g\pi {R_f}^2 \int_0^t \int_0^t x_f dt - (m_f + A)x_f \tag{13}$$

He data of float pendulum displacement and pendulum velocity versus corresponding time are substituted back into (12) (13) to obtain the graph of oscillator pendulum displacement and pendulum velocity versus corresponding time.

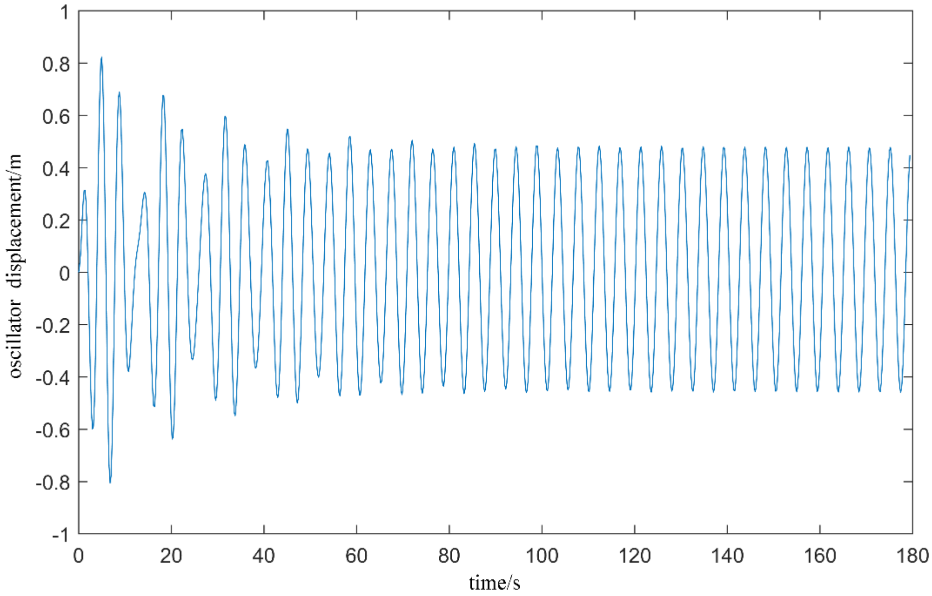

Figure 6. Plot of oscillator displacement versus time

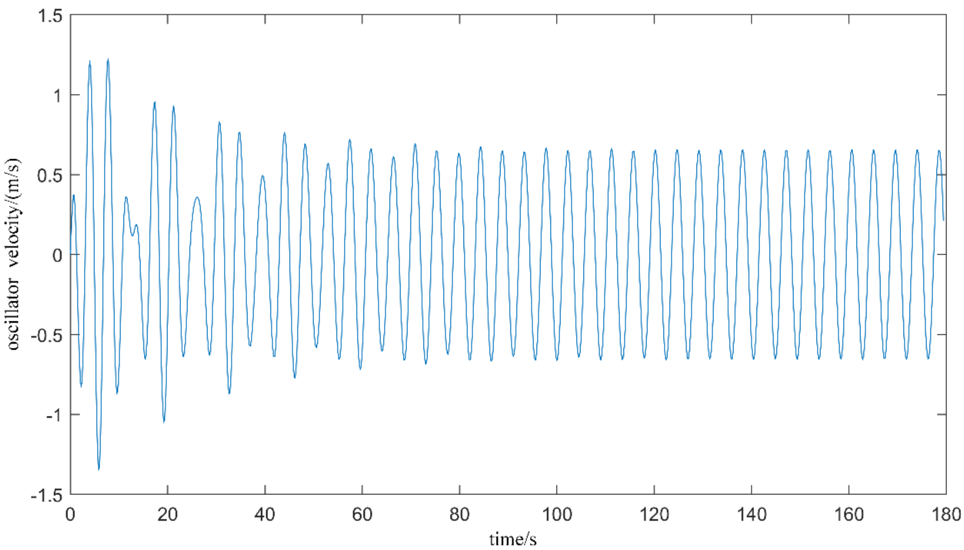

Figure 7. Plot of oscillator velocity versus time

And obtain the pendular displacement and velocity of the oscillator at 10 s, 20 s, 40 s, 60 s and 100 s.

Table 2. pendular displacement and velocity of the oscillator

Time	10s	20s	40s	60s	100s
oscillator displacement (m)	-0.1011	-0.5807	0.2591	-0.2416	0.0224
oscillator velocity (m/s)	-0.7159	-0.4088	0.4128	-0.5934	-0.6628

In this section, the damping factor of the linear damper is no longer equal to the proportionality factor above, but is proportional to the power of the absolute values of the relative velocities of the float and the oscillator, where the proportionality factor is taken to be 10000 and the power exponent is taken to be 0.5. Similar to question (1), the following two equations are listed based on the kinetic analysis of the float and the oscillator, respectively.

$$(m_f + A)\ddot{x_f} = f coswt - B\dot{x_f} - \rho g\pi {R_f}^2 x_f - C|\dot{x_f} - \dot{x_o}|^{\frac{1}{2}} \cdot (\dot{x_f} - \dot{x_o}) - k(x_f - x_o) \tag{14}$$

$$m_o\ddot{x_o} = C|\dot{x_f} - \dot{x_o}|^{\frac{1}{2}} \cdot (\dot{x_f} - \dot{x_o}) + k(x_f - x_o) \tag{15}$$

Combining these two equations, the following fourth-order ordinary differential equation for thex_f dual integral is obtained.

$$(m_f+A)\ddot{x_f}=fcoswt-B\dot{x_f}-\rho g\pi {R_f}^2x_f+C|\frac{1}{m_o}[\frac{f}{w}sinwt-Bx_f-\rho g\pi {R_f}^2\int_0^t x_fdt-(m_f+A+m_o)\dot{x_f}]|^{\frac{1}{2}}$$
$$\cdot\frac{1}{m_o}[\frac{f}{w}sinwt-Bx_f-\rho g\pi {R_f}^2\int_0^t x_fdt-(m_f+A+m_o)\dot{x_f}]+k\cdot\frac{1}{m_o}[-\frac{f}{w^2}coswt+\frac{f}{w^2} \tag{16}$$
$$-B\int_0^t x_fdt-\rho g\pi {R_f}^2\int_0^t\int_0^t x_fdt-(m_f+m_o+A)x_f]$$

Referring to the first question, list the system of Longuegutta equations.

$$\begin{cases} dy3=\ddot{x_f}=\frac{1}{m_f+A}\cdot\{fcoswt-B\dot{x_f}-\rho g\pi {R_f}^2x_f+C|\frac{1}{m_o}[\frac{f}{w}sinwt-Bx_f-\rho g\pi {R_f}^2\int_0^t x_fdt \\ \quad -(m_f+A+m_o)\dot{x_f}]|^{\frac{1}{2}}\cdot\frac{1}{m_o}[\frac{f}{w}sinwt-Bx_f-\rho g\pi {R_f}^2\int_0^t x_fdt-(m_f+A+m_o)\dot{x_f}] \\ \quad +k\cdot\frac{1}{m_o}[-\frac{f}{w^2}coswt+\frac{f}{w^2}-B\int_0^t x_fdt-\rho g\pi {R_f}^2\int_0^t\int_0^t x_fdt-(m_f+m_o+A)x_f]\} \\ dy2=\dot{x_f} \\ dy1=x_f \\ dy0=\int_0^t x_fdt \end{cases} \tag{17}$$

Similarly, starting from the initial time t = 0, setting the iteration step size to 0.1s, each iteration substitutes the t-value into the equation and calculates the corresponding $\dot{x_f}$ and x_f by programming the multi-value prediction, respectively, drawing the following images.

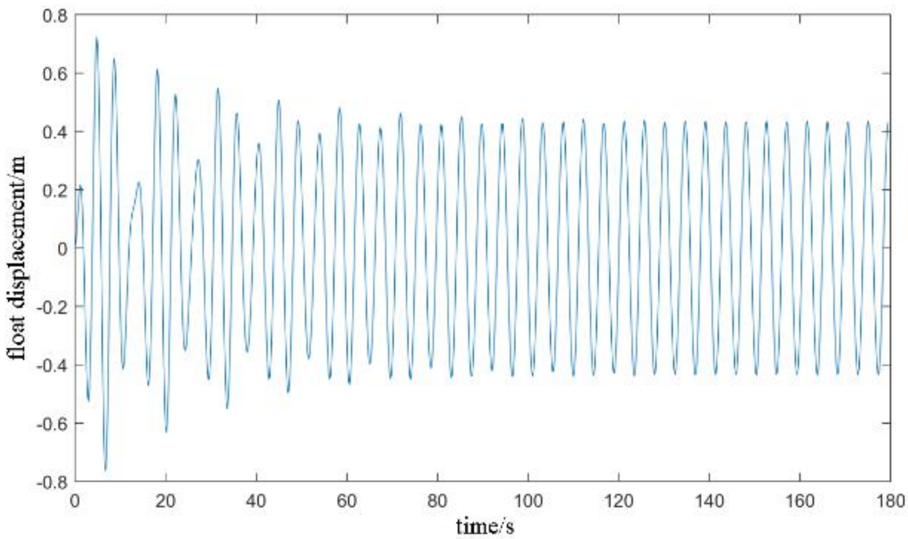

Figure 8. Plot of float displacement versus time

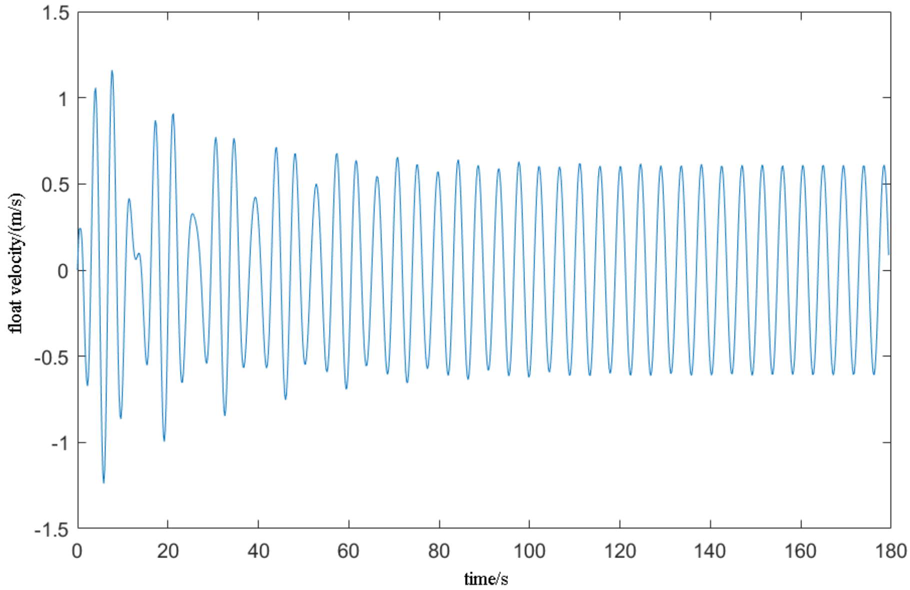

Figure 9. Plot of float velocity versus time

And The float displacement and velocity for 10 s, 20 s, 40 s, 60 s and 100 s are obtained.

Table 3. pendular displacement and velocity of the float

Time	10s	20s	40s	60s	100s
float displacement (m)	-0.2059	-0.6111	0.2688	-0.3272	-0.0884
float velocity (m/s)	-0.6528	-0.2548	0.2953	-0.4915	-0.6098

The relationship between oscillator displacement, velocity and float displacement is obtained from equation (12) (13), and by substituting the above float data, the following image of oscillator displacement and velocity about t can be obtained.

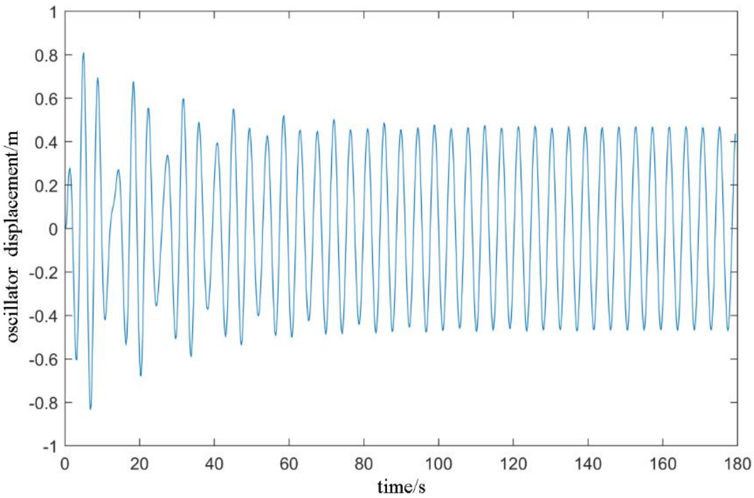

Figure 10. Plot of oscillator displacement versus time

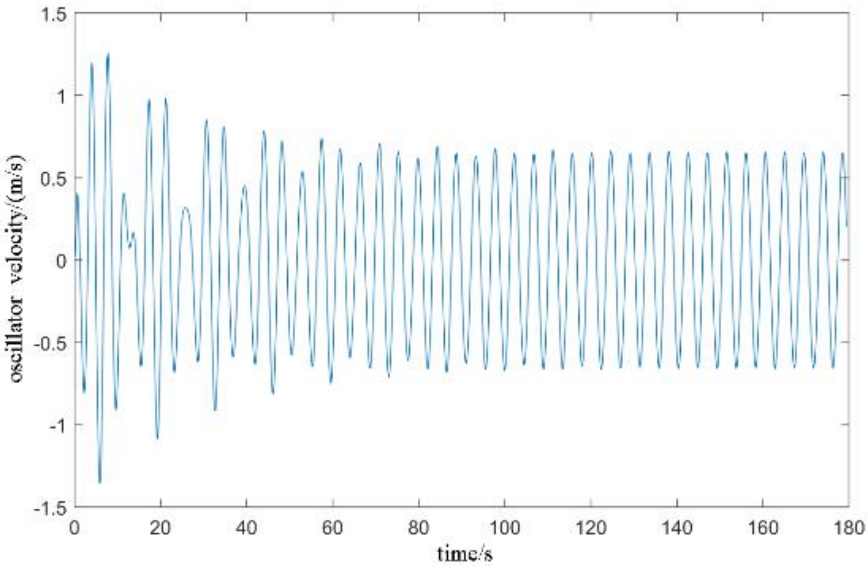

Figure 11. Plot of oscillator velocity versus time

And the pendulum displacement and velocity of the oscillator are obtained for 10 s, 20 s, 40 s, 60 s and 100 s.

Table 4. pendular displacement and velocity of the oscillator

Time	10s	20s	40s	60s	100s
oscillator displacement (m)	-0.1186	-0.6094	0.2227	-0.2605	0.0136
oscillator velocity (m/s)	-0.7516	-0.4349	0.3815	-0.6092	-0.6714

3. Model building and solution

3.1. Analysis of pendular motion

When the amplitude of longitudinal rocking motion is small, the angle of deviation of float and oscillator from vertical direction is small, and when they do pendular motion, the angle of force deflection in vertical direction is also small, which can be approximated as keeping vertical. Therefore, the above kinematic expressions of the pendular motion can be used. Finally, the angular displacement and angular velocity of the float oscillator are obtained as a function of time, and the pendular displacement and pendular velocity of the float oscillator are obtained for 10 s, 20 s, 40 s, 60 s, and 100 s.

Table 5. motion of float and oscillator

Time	10s	20s	40s	60s	100s
float displacement (m)	-0.5279	-0.7032	0.3709	-0.3199	-0.0501
float velocity (m/s)	0.9853	-0.2601	0.7600	-0.7215	-0.9468
oscillator displacement (m)	-0.6871	-0.7212	0.3186	-0.2504	0.0655
oscillator velocity (m/s)	0.9159	-0.4905	0.9419	-0.8803	-1.0474

According to the definition of rotational inertia and the parallel axis formula, the following calculation can be obtained. The rotational inertia of the top circular surface of the cylinder is as follows

$$J_1 = \frac{\sigma\pi {R_f}^4}{4} + \sigma\pi {R_f}^2 {h_2}^2 \tag{18}$$

The rotational inertia of the cylindrical column is shown below.

$$J_2 = \int_0^{h_2} \left(\sigma\pi {R_f}^3 + 2\sigma\pi R_f x^2\right) dx = \sigma\pi ({R_f}^3 h_2 + \frac{2}{3} R_f {h_2}^3) \tag{19}$$

The rotational inertia of the cone is shown below.

$$J_3 = \int_0^{h_1} (\sigma\pi r^3 + 2\sigma\pi r x^2) dx + \sigma\pi R_f \sqrt{{R_f}^2 + {h_1}^2} \cdot {h_1}^2 = \frac{\sigma\pi}{4} \left({R_f}^3 h_1 + R_f {h_1}^3\right) + \sigma\pi R_f \sqrt{{R_f}^2 + {h_1}^2} \cdot {h_1}^2 \tag{20}$$

From the above, the total rotational inertia of the float is

$$J_f = J_1 + J_2 + J_3 \tag{21}$$

Where, σ is the surface density of the float, calculated as

$$\sigma = \frac{m_f}{\pi {R_f}^2 + 2\pi R_f h_2 + \pi R_f \sqrt{{R_f}^2 + {h_2}^2}} \tag{22}$$

The oscillator is a solid column with uniformly distributed mass, and its location distribution inside the float is shown in the following figure 12.

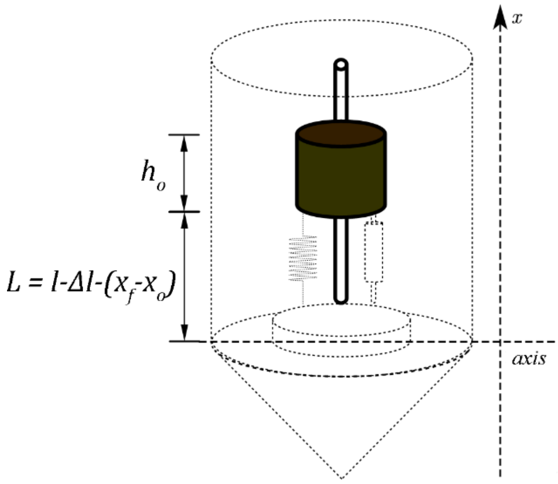

Figure 12. Structure of oscillator

The rotational inertia of the oscillator is as follows

$$\begin{aligned} J_z &= \int_0^{h_o} (\frac{1}{4}\rho\pi {R_o}^4 + \rho\pi\, {R_o}^2 x^2) dx + m_o \cdot [l - \Delta l - (x_f - x_o)^2] \\ &= \frac{1}{4}\rho\pi {R_o}^4 h_o + \frac{1}{3}\rho\pi {R_o}^2 {h_o}^3 + m_o \cdot [l - \Delta l - (x_f - x_o)^2] \end{aligned} \tag{23}$$

Where ρ is the bulk density of the oscillator, calculated as

$$\rho = \frac{m_o}{\pi {R_f}^2 h_o} \tag{24}$$

3.2. Analysis of longitudinal rocking motion

The schematic diagram of float and oscillator rotation is shown below. We specify counterclockwise rotation as positive and clockwise rotation as negative.

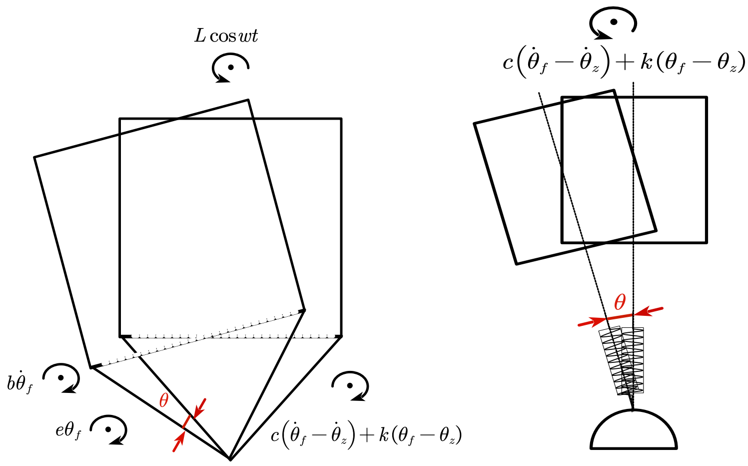

Figure 13. Analysis of float (left) and oscillator (right) rotation

According to the law of rigid body rotation and work by Xu et al. [10], the kinematic analysis of the external torque on the float and the rigid body rotation finally leads to the fourth order ordinary differential equation of θ_f about t.

$$(J_f + a)\theta_f^{(4)} = -Lw^2coswt - b\dddot{\theta}_f - e\ddot{\theta}_f - c(\dddot{\theta}_f - \dddot{\theta}_o) - k(\ddot{\theta}_f - \ddot{\theta}_o) \tag{25}$$

The angular displacement and angular velocity of the float oscillator are obtained as a function of time by solving the fourth-order ordinary differential equation using the Longacurta method as shown in figure 15 and figure 16 below:

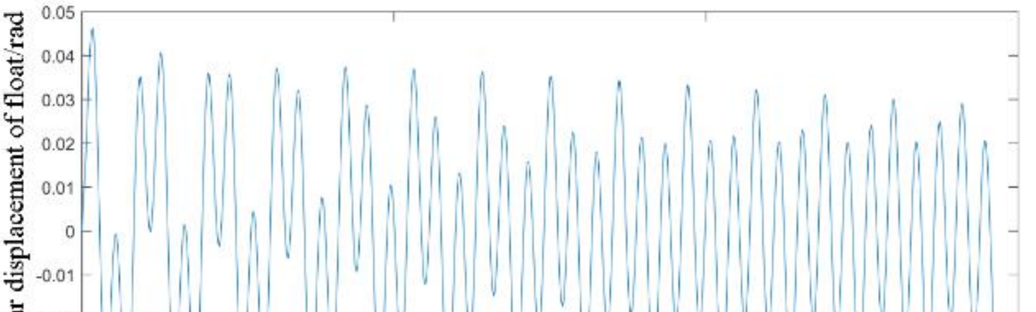

Figure 14. Plot of float longitudinal swing angular displacement vs. Time

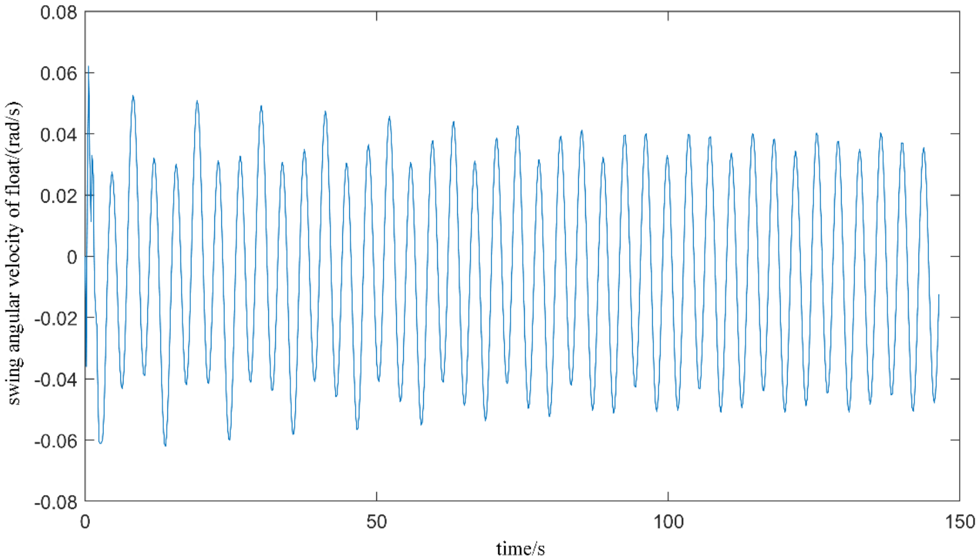

Figure 15. Plot of float longitudinal swing angular velocity vs. time

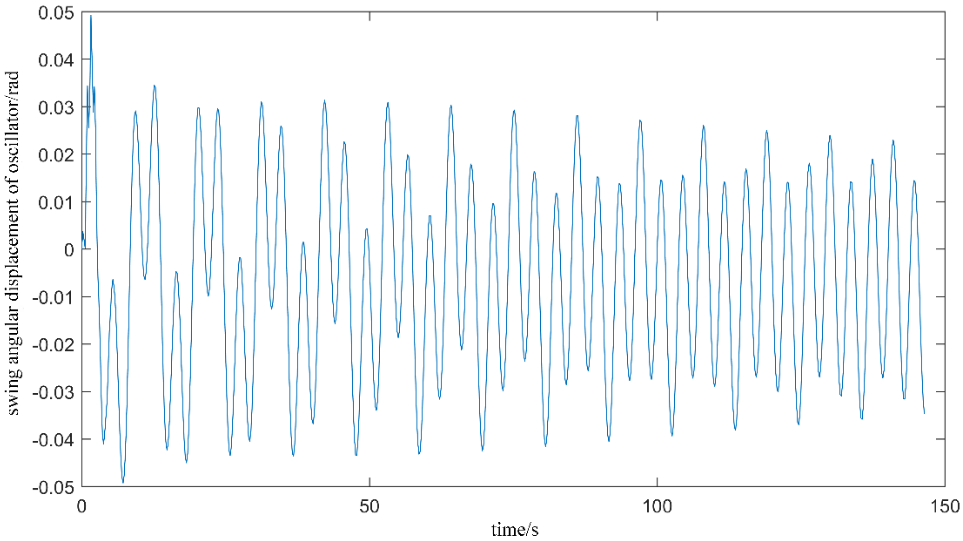

Figure 16. Longitudinal displacement of oscillator versus time

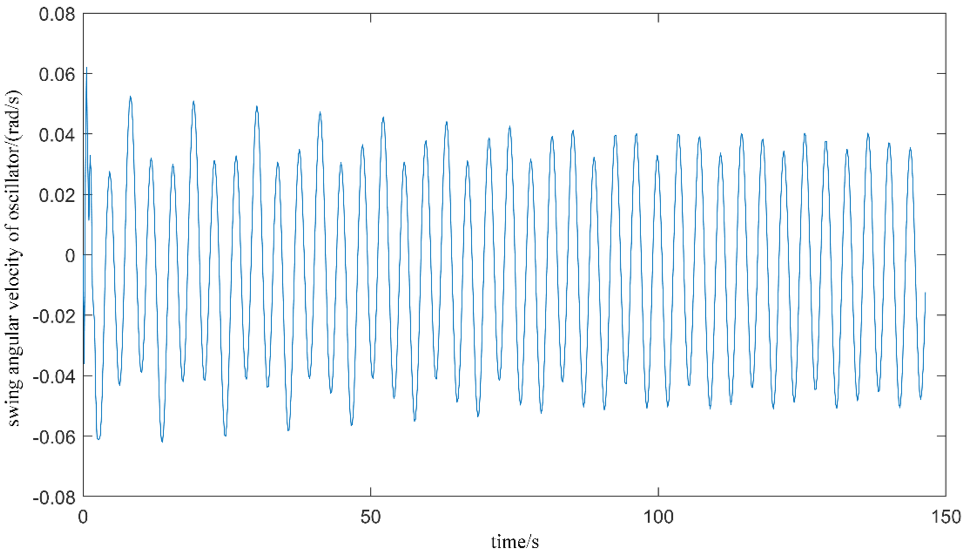

Figure 17. Longitudinal velocity of oscillator versus time

The longitudinal swing angular displacement and longitudinal swing angular velocity of the float and oscillator at 10 s, 20 s, 40 s, 60 s and 100 s are obtained.

Table 6. angular motion of float and oscillator

Time	10s	20s	40s	60s	100s
swing angular displacement of float(rad)	0.0220	0.0331	-0.0296	0.0053	0.0068
swing angular velocity of float(rad/s)	-0.0383	0.0169	-0.0161	0.0262	0.0308
swing angular displacement of oscillator (rad)	0.0161	0.0267	-0.0358	-0.0011	0.0003
swing angular velocity of oscillator (rad/s)	-0.0463	0.0084	-0.0255	0.0176	0.0221

4. Conclusion

The dynamic analysis model of the wave energy device is constructed in this paper to analyze the dynamics of the pendular and longitudinal oscillation motion of the float and oscillator in the device respectively. Compared with the real situation, the wave energy device will not only make vertical and longitudinal oscillation motion, but also make transverse oscillation motion at sea level. The problem is simplified and no requirements are made for this case. And there will also be non-periodic external forces such as sea breeze on the sea surface that will cause the model to oscillate. All these factors should be taken into account if the model is put into practical use.

References

[1] Zhao JF, Huang XY, Chen L. Wave energy generation technology and research status [J]. Hunan Water Conservancy and Hydropower, 2022 (03): 7 - 11. DOI: 10.16052/j.cnki.hnslsd.2022.03.030.

[2] LU Kuan, WANG Huamei, HAN Linsheng. Research on the incident wave power calculation method in the laboratory of wave energy generation device model under irregular waves[J]. Journal of Solar Energy, 2020, 41 (08): 36 - 40. DOI: 10.19912/j.0254-0096.2020.08.006.

[3] Wu BJ, Zhang FM, Long ZX, Li M, Wu RK. Self-propelled pneumatic oscillating water column wave energy generation vessel technology[J]. Journal of Solar Energy,2022, 43 (08): 458 - 462. DOI: 10.19912/j.0254 - 0096.tynxb.2021 - 0057.

[4] Xie, Huimei, Meng, Fantai, Xu, Qianlong, Wang, Shangming, Xie, Bin, Li, Ye. Performance analysis of multi-degree-of-freedom built-in PTO-type wave energy conversion devices with different shapes [J]. Renewable Energy,2022,40(07): 986-994.DOI: 10.13941/j.cnki.21 - 1469/tk.2022.07.004.

[5] Chen J, Lan F, Guo Hao-Lin, Lai JH. A review of wave energy generation control technology research [J/OL]. Power Automation Equipment:1-20 [2022-11-23]. DOI: 10.16081/j.epae.202208025.

[6] Ma, Zhe. Hydrodynamic characterization of oscillating float type wave power generation device [D]. Ocean University of China, 2013.

[7] Gao, Lang, Zhu, Liang-Sheng, Wang, Lei, Zhou, Bin-Zhen. Research on the hydrodynamic performance of the integrated system of pendulous wave energy device and wind turbine platform [J]. Guangdong Shipbuilding,2022, 41 (03): 17 - 21.

[8] Liu K. A fully implicit Taylor and Longacurta numerical method for solving stochastic differential equations [D]. Shanghai University of Finance and Economics, 2021. doi: 10.27296/d.cnki.gshcu.2021.001499.

[9] Shi JL. Research on wave energy generation device driven by inertia [D]. Nanjing University of Information Engineering, 2022. DOI: 10.27248/d.cnki.gnjqc.2022.000910.

[10] Xu L, Deng SZ, Xiong BK, Chen QC. Research on hydrodynamic performance of active resonant buoyant pendulum wave energy generation device [J]. Journal of Marine Technology, 2022, 41 (03): 90 - 96.